

ortho-Substituted azoles as selective and dual inhibitors of VEGF receptors 1 and 2

Alexander S. Kiselyov,^a Evgueni L. Piatnitski,^b Alexander V. Samet,^b
Victor P. Kisliy^b and Victor V. Semenov^{b,*}

^aSmall Molecule Drug Discovery, Chemical Diversity, Inc., 11558 Sorrento Valley Road, San Diego, CA 92121, USA

^bZelinsky Institute of Organic Chemistry, Russian Academy of Sciences, 47 Leninsky Prospect, 117913 Moscow, Russia

Received 16 October 2006; revised 18 November 2006; accepted 30 November 2006

Available online 2 December 2006

Abstract—We have developed a series of novel potent *ortho*-substituted azole derivatives active against kinases VEGFR-1 and VEGFR-2. Both specific and dual ATP-competitive inhibitors of VEGFR-2 were identified. Kinase activity and selectivity could be controlled by varying the arylamido substituents at the azole ring. The most specific molecule (**17**) displayed >10-fold selectivity for VEGFR-2 over VEGFR-1. Compound activities in enzymatic and cell-based assays were in the range of activities for reported clinical and development candidates (IC₅₀ < 100 nM), including Novartis' PTK787 (*Vatalanib*)TM. High permeability of active compounds across the Caco-2 cell monolayer (>30 × 10⁻⁵ cm/min) is indicative of their potential for intestinal absorption upon oral administration.

© 2007 Published by Elsevier Ltd.

Angiogenesis, or formation of new blood vessels, is a highly complex process. Proliferation and migration of capillary endothelial cells from pre-existing blood vessels is followed by tissue infiltration and cell assembly into tubular structures, joining of newly formed tubular assemblies to closed-circuit vascular systems, and maturation of newly formed capillary vessels. Angiogenesis is involved in pathological conditions such as tumor growth and degenerative eye conditions.¹ A family of vascular endothelial growth factors (VEGFs),² endothelial cell-specific mitogens, has been implicated in regulation of angiogenesis *in vivo*. VEGFs mediate their biological effect through high-affinity VEGF receptors that are expressed on the endothelial cells. These include receptor tyrosine kinases, VEGFR-1 (Flt-1) and VEGFR-2 (Kinase Insert Domain Receptor (KDR) or flk1).³ Whereas VEGFR-1 functions are still under investigation, there is substantial evidence that KDR is a major mediator of vascular endothelial cell mitogenesis as well as angiogenesis and microvascular permeability. It is believed that a direct inhibition of the aberrant

KDR kinase activity results in reduction of tumor angiogenesis and suppression of tumor growth. Potent, specific, and non-toxic inhibitors of angiogenesis are powerful clinical tools in oncology and ophthalmology.³

There are reports describing small-molecule inhibitors that affect VEGF/VEGFR signaling by directly competing with the ATP binding site of the respective intracellular kinase domain. This event leads to the inhibition of VEGFR phosphorylation and, ultimately, to the apoptotic death of the aberrant endothelial cells. Drug candidates that exhibit this mechanism of action include Novartis' PTK787 (*Vatalanib*)TM (**A**) and Astra-Zeneca's ZD6474 (*Vandetanib*)TM (**B**). These compounds are reported to be undergoing Phase III and Phase II clinical trials, respectively, for various oncology indications.^{4,5} The pyridazine ring of phthalazine template in PTK787 **A** has been replaced with the isosteric anthranil amide derivatives **C** and **D** (Fig. 1). Intramolecular hydrogen bonding was suggested to be responsible for the optimal spatial orientation of pharmacophore pieces, similar to the one of parent PTK787.⁶

It has been proposed that the essential pharmacophore elements for the VEGFR-2 activity of PTK787 type phthalazines and their analogs include (i) [6,6] fused (or related) aromatic system; (ii) *para*- or 3,4-*di*-substituted

Keywords: Vascular endothelial growth factor receptor; KDR; VEGFR-2; VEGFR-1; Receptor tyrosine kinase; Dual kinase inhibitors; Angiogenesis.

*Corresponding author. Tel.: +7 617 551 3302; e-mail: semenovictor@gmail.com

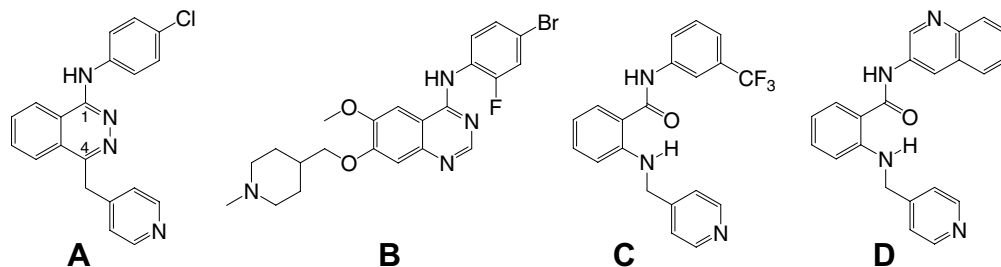


Figure 1. PTK787 (A), ZD6474 (B), and anthranilamide derivatives (C, D).

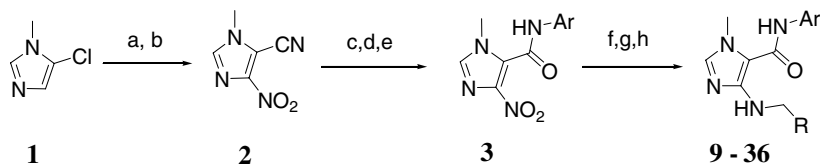
aniline at position 1 of phthalazine core; (iii) hydrogen bond acceptor (Lewis' base: lone pair(s) of a nitrogen- or oxygen atom(s)) attached to the position 4 via an appropriate linker (aryl or fused aryl group).⁴ In this communication, we expand upon our initial findings⁷ and disclose potent inhibitors of VEGFR-2 kinase based on *ortho*-substituted azoles. We reasoned that these non-phthalazine templates could provide for a proper pharmacophore arrangement consistent with the model proposed for PTK787.^{4,6}

Our synthetic route to imidazole derivatives (**9–36**) is illustrated in Scheme 1. Nitration of *N*-methyl 5-chloroimidazole (**1**) with a 1:1 mixture of HNO₃/H₂SO₄ yielded the expected 4-nitro derivative in 91% yield. This was treated with KI/KCN (10-fold excess) mixture in EtOH at reflux for 12 h to result in the product of formal substitution of chlorine with nitrile (**2**, 69% yield). Product (**2**) was subsequently hydrolyzed to the corresponding acid followed by its conversion into acyl chloride and a coupling with a series of anilines leading to intermediates (**3**) in 39–67% yield over three-steps. Reduction of NO₂ functionality into a corresponding amine followed by its reaction with various aldehydes to furnish Schiff bases and their reduction with NaBH₄ in *i*-PrOH afforded the desired imidazoles (**9–36**) (59–75% yield over three steps). In the next series of experiments, we prepared pyrazole derivatives with a similar substituent arrangement (Scheme 2). Acid (**4**) was methylated into a mixture of two regioisomeric *N*-pyrazoles (ratio of 1-Me to 2-Me products was ca. 1:1). These compounds were separated by crystallization and nitrated with a 1:1 mixture of HNO₃ and H₂SO₄ (a respective scheme for 1-Me isomer is shown) to yield the corresponding 4-nitro-5-carboxy pyrazole (**5**) (77% yield for the three step sequence). Pyrazole (**5**) was then converted into a series of *ortho*-substituted derivatives (**37–60**) via the same sequence reported above for the synthesis of imidazoles. The desired pyrazoles were isolated in 37–56% yield starting from (**5**). Syntheses of the corresponding *ortho*-substituted isoxazole derivatives (**61–78**) were accomplished starting with ethyl cyanoacetate as reported in the literature (Scheme 3).⁸ The targeted structures (**61–78**) were prepared in 41–63% overall yields starting from (**6**). Notably, all three protocols were amendable for scale up to produce multi-gram quantities of compounds (**9–78**).⁹

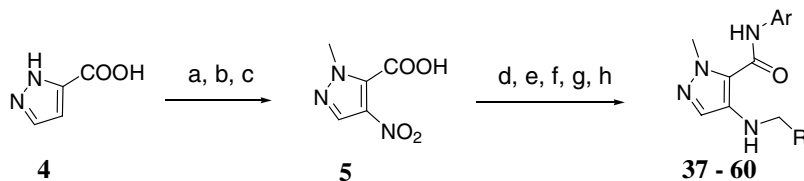
Compounds (**9–78**, Table 1) were tested *in vitro* against isolated VEGFR-2 kinase. Specifically, we measured

their ability to inhibit phosphorylation of a biotinylated polypeptide substrate (*p*-GAT, *CIS Bio International*) in a homogeneous time-resolved fluorescence (HTRF) assay at ATP concentration of 2 μM. Literature-reported VEGFR-2 inhibitors **A–D** (Table 1) were included as internal standards for quality control.⁷ As it is shown in Table 1, a number of azole β-amino acid amides exhibited a robust inhibitory activity against VEGFR-2. By varying both anilide substituents and aryl methylamino tailpiece, we modulated compound potency against the enzyme. Initial experiments in the imidazole series (entries **9–13**, Table 1) suggested that pyridin-4-ylmethylamino substituent yields the best activity with the enzymatic IC₅₀ value of 650 nM against VEGFR-2 (**13**). The activity against VEGFR-1 followed the same trend with pyridin-4-ylmethylamino analog giving the lowest IC₅₀ value in enzymatic assay. These results were somewhat disappointing since the corresponding 6-membered analog **C** in our internal enzymatic VEGFR-2 assay showed much better potency (IC₅₀ = 32 nM). The respective analog (**24**) for compound **D** displayed enzymatic potency of 230 nM in enzymatic assay compared to 10-fold higher activity for the compound **D** (IC₅₀ = 23 nM). We decided to further investigate the effect of aniline group on the compound activity within imidazole series. Substituents in the aniline ring were widely varied as well as the entire aniline moiety being replaced with bicyclic groups (**24–26**). It was observed that *t*-Bu group (**19**) gave the highest enzymatic activity (IC₅₀ = 87 nM). Larger anilinic substituents led to the diminished potency against the enzyme (**21–23**, **49–51**, **70–72**). Specifically, *para*-phenyl-, phenoxy-, and benzyl-derivatives showed weak to no enzymatic activity. We speculated that these functions could not be properly accommodated in the tight hydrophobic pocket of VEGFR-2.¹⁰

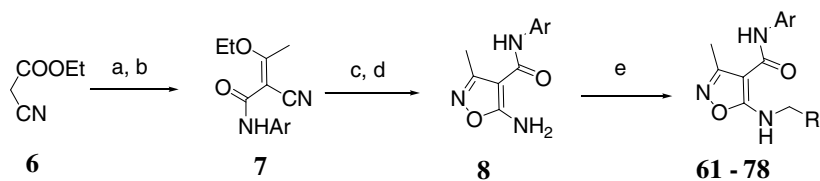
Compounds (**9–78**) were also tested via HTRF format against VEGFR-1. The results in Table 1 indicate that many VEGFR-2 active ((pyridin-4-yl)ethyl)pyridines display good activity against VEGFR-1 as well. For the most potent compounds, the IC₅₀ values were reaching 0.11 μM in the enzymatic assay. This outcome could be of benefit in the clinical setting as both receptors are reported to mediate VEGF signaling in angiogenesis.¹¹ One particular imidazole compound (**17**) yielded over 10-fold selectivity for the VEGFR-2 versus VEGFR-1 kinase providing us with a rare example of such selectivity between these closely related targets. Notably, a corresponding pyrazole analog also displayed some



Scheme 1. Reagents and conditions: (a) HNO₃, H₂SO₄, H₂O, heat; (b) KCN, KI, EtOH, reflux; (c) H₂O, H₂SO₄, heat; (d) SOCl₂, reflux; (e) ArNH₂, Et₃N; (f) H₂, Pd/C, EtOAc/DMF; (g) RCHO, MeOH; (h) NaBH₄, *i*-PrOH, reflux.



Scheme 2. Reagents and conditions: (a) Me₂SO, aq. NaOH; (b) Crystallization; (c) H₂SO₄, HNO₃, heat; (d) SOCl₂, reflux; (e) ArNH₂, Et₃N; (f) H₂, Pd/C, EtOAc; (g) RCHO, MeOH; (h) NaBH₄, *i*-PrOH, reflux.



Scheme 3. Reagents and conditions: (a) ArNH₂, imidazole, EtOH, 200 °C; (b) Et(OEt)₃, Ac₂O, reflux; (c) NH₂OH HCl, KOH, MeOH, 60 °C; (d) RCHO, *p*-TsOH, *i*-PrOH; (e) NaBH₄, *i*-PrOH.

selectivity, but with the lower VEGFR-2 activity. These observations suggest that it is possible to develop VEGFR-2-specific inhibitors lacking VEGFR-1 cross-reactivity. Structural reasons for this VEGFR-2 specificity are under further investigation. Screening of **59–78** against a number of other receptors (IGF1R, InR, FGFR1, Flt3, ErbB1, ErbB2, c-Met) and cytosolic (PKA, GSK3 β , PKB/Akt, bcr-Abl, Cdk2, Cdk5) kinases revealed no significant cross-reactivity ($PI < 30\%$, triplicate measurements) at a screening concentration of 10 μ M.

In general, we have observed good SAR correlations amongst the imidazole, pyrazole, and isoxazole scaffolds. The most active compounds in each series contained *t*-Bu group in *para*-position ((**19**), (**47**), (**68**)). Nevertheless, a few exceptions were also found where substituents favored in one template gave no activity in another azole class (compare (**17**, **18**), (**45**, **46**) to (**66**, **67**)). On average, VEGFR-2 enzymatic potency somewhat decreased in the following order: imidazoles > pyrazoles > isoxazoles. We also explored several variations in imidazole, pyrazole, and isoxazole heterocycles. 2-Substituted imidazoles (R = Me, Et, Pr, Scheme 4) were prepared in 28–44% total yields as described below. The resulting compounds were inactive against both VEGFR-2 and VEGFR-1 ($PI < 30\%$ at 10 μ M). The methyl group at position 3 of isoxazole template was also modified using a similar protocol described in Scheme 3. 3-Ethyl and 3-propyl substituted isoxazoles proved to be inactive for both targets. We have also expanded our studies to various isomeric pyr-

azoles. These efforts and the findings will be discussed in details in upcoming publications. It was determined that the above-mentioned 4-amino-1-methyl-1*H*-pyrazole-5-carboxamide motif resulted in optimal VEGFR-2 activity. Moreover, once the methyl group on pyrazole nitrogen was removed to give unsubstituted pyrazole nitrogen, the activity of the molecule against both targets dropped significantly.

Good inhibitory activity of the compounds containing pyridin-4-ylmethylamino group (compare (**9**) to (**13**), (**37**) to (**41**)) was explained by a proper alignment of the 4-substituent, namely pyridine-type nitrogen atom (Lewis' base: hydrogen bond acceptor) with the Arg1302 moiety in the ATP-binding pocket of VEGFR-2.¹⁰ We further reasoned that in (**9**) and (**37**) the nitrogen of the pyridine ring and the lone pairs of the methylenedioxy group in the piperonal derivatives (**10**, **11**, **38**, and **39**) are likely to be mis-aligned with the Arg1302.¹⁰ MMFF94 Force Field minimization studies suggested a good overlap between the active series described in this paper and the development candidates PTK787 and **C** where the interactions with Arg1302 were well described in the literature (Fig. 2). Following these data, we decided to continue optimization of the molecules derived from 4-pyridyl aldehyde (**13–36**, **41–78**, Table 1).

Inhibitors of VEGFR-2 active *in vitro* were further characterized in a cell-based phosphorylation ELISA (Table 1).⁷ In general, good enzymatic-to-cell-based activity correlation has been found for these

Table 1. Activity of azole β -amino acid amides (**9–78**) against VEGFR-1 and VEGFR-2 tyrosine kinases

Azoles
Imid (9-36)
Pyraz (37-60)
Isoxaz (61-78)

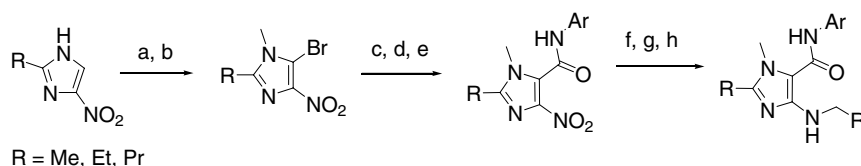
Compound	Azole	Ar	R	VEGFR-2, enzymatic, IC ₅₀ ^a (μM)	VEGFR-1, enzymatic, IC ₅₀ ^a μM	VEGFR-2, cellular ELISA, IC ₅₀ ^{a,b} (μM)
A, PTK787				0.054 ± 0.006 (0.042 ± 0.003) ^{6a}	0.14 ± 0.02 (0.11 ± 0.03) ^{6a}	0.021 ± 0.03 (0.016 ± 0.001) ^{6a}
B, ZD6474				0.022 ± 0.003 (0.017 ± 0.003) ^{6a}	0.10 ± 0.01 (0.09 ± 0.01) ^{6a}	1.66 ± 0.11 (2.70 ± 0.17) ^{6a}
C				0.032 ± 0.005 (0.023 ± 0.006) ^{6a}	0.17 ± 0.05 (0.130 ± 0.081) ^{6a}	0.09 ± 0.01 (0.0012 ± 0.0002) ^{6a}
D				0.015 ± 0.004 (0.009 ± 0.001) ^{6a}	0.16 ± 0.05 (0.13 ± 0.03) ^{6a}	0.05 ± 0.01 (0.0012 ± 0.0001) ^{6a}
9	<i>Imid</i>	3-F ₃ C(C ₆ H ₄)	3-Pyridine	>10	>10	>10
10	<i>Imid</i>	3-F ₃ C(C ₆ H ₄)	3,4-Piperonyl	2.27 ± 0.41	3.12 ± 0.55	>10
11	<i>Imid</i>	4-F ₃ C(C ₆ H ₄)	3,4-Piperonyl	1.68 ± 0.30	2.55 ± 0.44	>10
12	<i>Imid</i>	4-F ₃ C(C ₆ H ₄)	3-Pyridine	>10	>10	>10
13	<i>Imid</i>	3-F ₃ C(C ₆ H ₄)	4-Pyridine	0.65 ± 0.08	0.79 ± 0.11	0.55 ± 0.07
14	<i>Imid</i>	4-F ₃ C(C ₆ H ₄)	4-Pyridine	1.98 ± 0.35	6.00 ± 0.16	9.60 ± 1.70
15	<i>Imid</i>	4-F ₃ CO(C ₆ H ₄)	4-Pyridine	1.15 ± 0.12	1.43 ± 0.12	0.11 ± 0.01
16	<i>Imid</i>	3-F ₃ CO(C ₆ H ₄)	4-Pyridine	0.76 ± 0.09	1.11 ± 0.10	0.35 ± 0.05
17	<i>Imid</i>	4-Cl(C ₆ H ₄)	4-Pyridine	0.25 ± 0.10	>10	1.65 ± 0.19
18	<i>Imid</i>	3-Cl(C ₆ H ₄)	4-Pyridine	2.06 ± 0.21	3.22 ± 0.36	>10
19	<i>Imid</i>	4- <i>t</i> Bu(C ₆ H ₄)	4-Pyridine	0.087 ± 0.008	0.11 ± 0.01	0.064 ± 0.005
20	<i>Imid</i>	4- <i>i</i> Pr(C ₆ H ₄)	4-Pyridine	0.18 ± 0.02	0.27 ± 0.04	0.075 ± 0.007
21	<i>Imid</i>	4-Ph(C ₆ H ₄)	4-Pyridine	3.77 ± 0.56	>10	>10
22	<i>Imid</i>	4-PhO(C ₆ H ₄)	4-Pyridine	4.29 ± 0.61	>10	>10
23	<i>Imid</i>	4-Bn(C ₆ H ₄)	4-Pyridine	5.57 ± 0.72	>10	>10
24	<i>Imid</i>	3-(Quinoliny)	4-Pyridine	0.23 ± 0.01	0.35 ± 0.04	0.92 ± 0.09
25	<i>Imid</i>	5-(Indazolyl)	4-Pyridine	6.02 ± 0.77	>10	>10
26	<i>Imid</i>	6-(Indazolyl)	4-Pyridine	5.73 ± 0.69	>10	>10
27	<i>Imid</i>	3-CF ₃ ,4-Cl(C ₆ H ₄)	4-Pyridine	0.95 ± 0.044	1.26 ± 0.11	0.17 ± 0.02
28	<i>Imid</i>	3-Cl,4-CF ₃ (C ₆ H ₄)	4-Pyridine	0.29 ± 0.02	0.35 ± 0.06	0.088 ± 0.008
29	<i>Imid</i>	3,4-di-Cl(C ₆ H ₄)	4-Pyridine	0.37 ± 0.05	0.55 ± 0.09	0.096 ± 0.007
30	<i>Imid</i>	3,4-di-MeO(C ₆ H ₄)	4-Pyridine	0.21 ± 0.03	0.35 ± 0.04	0.057 ± 0.008
31	<i>Imid</i>	3,4-di-CF ₃ (C ₆ H ₄)	4-Pyridine	0.58 ± 0.08	0.69 ± 0.10	0.11 ± 0.01
32	<i>Imid</i>	3,5-di-CF ₃ (C ₆ H ₄)	4-Pyridine	0.74 ± 0.09	1.06 ± 0.11	0.15 ± 0.02
33	<i>Imid</i>	4-Me-3-CF ₃ (C ₆ H ₃)	4-Pyridine	0.34 ± 0.05	0.61 ± 0.07	0.089 ± 0.01
34	<i>Imid</i>	3-Me-4-CF ₃ (C ₆ H ₃)	4-Pyridine	0.21 ± 0.02	0.51 ± 0.07	0.064 ± 0.007
35	<i>Imid</i>	2-F-4-Me(C ₆ H ₃)	4-Pyridine	0.84 ± 0.08	1.35 ± 0.18	1.25 ± 0.11
36	<i>Imid</i>	3,4-Piperonyl	4-Pyridine	0.65 ± 0.07	1.12 ± 0.11	0.74 ± 0.08
37	<i>Pyraz</i>	3-F ₃ C(C ₆ H ₄)	3-Pyridine	>10	>10	>10
38	<i>Pyraz</i>	3-F ₃ C(C ₆ H ₄)	3,4-Piperonyl	5.29 ± 0.56	>10	>10
39	<i>Pyraz</i>	4-F ₃ C(C ₆ H ₄)	3,4-Piperonyl	>10	>10	>10
40	<i>Pyraz</i>	4-F ₃ C(C ₆ H ₄)	3-Pyridine	>10	>10	>10
41	<i>Pyraz</i>	3-F ₃ C(C ₆ H ₄)	4-Pyridine	0.75 ± 0.12	1.06 ± 0.15	1.34 ± 0.10
42	<i>Pyraz</i>	4-F ₃ C(C ₆ H ₄)	4-Pyridine	0.28 ± 0.02	0.31 ± 0.04	0.13 ± 0.01
43	<i>Pyraz</i>	4-F ₃ CO(C ₆ H ₄)	4-Pyridine	0.73 ± 0.08	1.87 ± 0.21	0.064 ± 0.009
44	<i>Pyraz</i>	3-F ₃ CO(C ₆ H ₄)	4-Pyridine	2.06 ± 0.09	2.44 ± 0.32	0.47 ± 0.06
45	<i>Pyraz</i>	4-Cl(C ₆ H ₄)	4-Pyridine	4.58 ± 0.62	>10	1.00 ± 0.32
46	<i>Pyraz</i>	3-Cl(C ₆ H ₄)	4-Pyridine	2.06 ± 0.21	3.22 ± 0.36	>10
47	<i>Pyraz</i>	4- <i>t</i> Bu(C ₆ H ₄)	4-Pyridine	0.13 ± 0.01	0.18 ± 0.02	0.045 ± 0.005
48	<i>Pyraz</i>	4- <i>i</i> Pr(C ₆ H ₄)	4-Pyridine	0.29 ± 0.04	0.44 ± 0.05	0.088 ± 0.011
49	<i>Pyraz</i>	4-Ph(C ₆ H ₄)	4-Pyridine	>10	>10	>10
50	<i>Pyraz</i>	4-PhO(C ₆ H ₄)	4-Pyridine	>10	>10	>10
51	<i>Pyraz</i>	4-Bn(C ₆ H ₄)	4-Pyridine	5.57 ± 0.72	>10	>10
52	<i>Pyraz</i>	3-(Quinoliny)	4-Pyridine	0.28 ± 0.04	0.52 ± 0.08	1.14 ± 0.21
53	<i>Pyraz</i>	3-CF ₃ ,4-Cl(C ₆ H ₄)	4-Pyridine	1.13 ± 0.14	1.36 ± 0.10	0.11 ± 0.01
54	<i>Pyraz</i>	3-Cl,4-CF ₃ (C ₆ H ₄)	4-Pyridine	0.21 ± 0.03	0.44 ± 0.05	0.079 ± 0.007

Table 1 (continued)

Compound	Azole	Ar	R	VEGFR-2, enzymatic, IC ₅₀ ^a (μM)	VEGFR-1, enzymatic, IC ₅₀ ^a (μM)	VEGFR-2, cellular ELISA, IC ₅₀ ^{a,b} (μM)
55	<i>Pyraz</i>	3,4-di-Cl(C ₆ H ₄)	4-Pyridine	0.25 ± 0.04	0.36 ± 0.05	0.082 ± 0.009
56	<i>Pyraz</i>	3,4-di-MeO(C ₆ H ₄)	4-Pyridine	0.35 ± 0.05	0.51 ± 0.07	0.091 ± 0.012
57	<i>Pyraz</i>	3,4-di-CF ₃ (C ₆ H ₄)	4-Pyridine	0.84 ± 0.10	0.92 ± 0.11	0.13 ± 0.02
58	<i>Pyraz</i>	3,5-di-CF ₃ (C ₆ H ₄)	4-Pyridine	1.12 ± 0.15	1.23 ± 0.09	0.21 ± 0.04
59	<i>Pyraz</i>	4-Me-3-CF ₃ (C ₆ H ₃)	4-Pyridine	0.66 ± 0.08	0.93 ± 0.11	0.102 ± 0.009
60	<i>Pyraz</i>	3-Me-4-CF ₃ (C ₆ H ₃)	4-Pyridine	0.33 ± 0.05	0.56 ± 0.09	0.069 ± 0.008
61	<i>Isoxaz</i>	3-F ₃ C(C ₆ H ₄)	4-Pyridine	1.56 ± 0.14	1.69 ± 0.15	2.27 ± 0.35
62	<i>Isoxaz</i>	4-F ₃ C(C ₆ H ₄)	4-Pyridine	0.37 ± 0.05	0.56 ± 0.08	0.18 ± 0.02
63	<i>Isoxaz</i>	4-F ₃ CO(C ₆ H ₄)	4-Pyridine	2.12 ± 0.21	3.55 ± 0.32	0.91 ± 0.01
64	<i>Isoxaz</i>	3-F ₃ CO(C ₆ H ₄)	4-Pyridine	5.66 ± 0.64	>10	>10
65	<i>Isoxaz</i>	4-Cl(C ₆ H ₄)	4-Pyridine	>10	>10	>10
66	<i>Isoxaz</i>	3-Cl(C ₆ H ₄)	4-Pyridine	>10	>10	>10
67	<i>Isoxaz</i>	4- <i>t</i> Bu(C ₆ H ₄)	4-Pyridine	0.28 ± 0.05	0.42 ± 0.07	0.21 ± 0.03
68	<i>Isoxaz</i>	4- <i>i</i> Pr(C ₆ H ₄)	4-Pyridine	0.44 ± 0.09	0.76 ± 0.11	0.35 ± 0.04
69	<i>Isoxaz</i>	4-Ph(C ₆ H ₄)	4-Pyridine	>10	>10	>10
70	<i>Isoxaz</i>	4-PhO(C ₆ H ₄)	4-Pyridine	>10	>10	>10
71	<i>Isoxaz</i>	4-Bn(C ₆ H ₄)	4-Pyridine	5.80 ± 0.90	>10	>10
72	<i>Isoxaz</i>	3-(Quinoliny)	4-Pyridine	0.94 ± 0.15	1.22 ± 0.13	3.54 ± 0.67
73	<i>Isoxaz</i>	3-CF ₃ ,4-Cl(C ₆ H ₄)	4-Pyridine	3.27 ± 0.48	>10	>10
74	<i>Isoxaz</i>	3-Cl,4-CF ₃ (C ₆ H ₄)	4-Pyridine	0.56 ± 0.73	1.11 ± 0.15	0.32 ± 0.06
75	<i>Isoxaz</i>	3,4-di-Cl(C ₆ H ₄)	4-Pyridine	0.97 ± 0.14	1.25 ± 0.16	0.93 ± 0.11
76	<i>Isoxaz</i>	3,4-di-MeO(C ₆ H ₄)	4-Pyridine	1.19 ± 0.17	3.35 ± 0.44	>10
77	<i>Isoxaz</i>	3,4-di-CF ₃ (C ₆ H ₄)	4-Pyridine	4.23 ± 0.58	>10	>10
78	<i>Isoxaz</i>	3-Me-4-CF ₃ (C ₆ H ₃)	4-Pyridine	0.87 ± 0.09	1.44 ± 0.16	0.59 ± 0.08

^a IC₅₀ values were determined from the logarithmic concentration-inhibition curves (10 points). The values are given as mean of at least two duplicate experiments.

^b Compounds with cellular activities <100 nM are marked in bold italics.



Scheme 4. Reagents and conditions: (a) Br₂, aq. NaOH; (b) (CH₃)₂SO₂, aq. NaOH; (c) KCN, KI, EtOH, reflux; (d) H₂O, H₂SO₄, heat; (e) SOCl₂, refl.; ArNH₂, Et₃N; (f) H₂, Pd/C, EtOAc/DMF; (g) R'CHO, MeOH; (h) NaBH₄, *i*-PrOH, reflux.

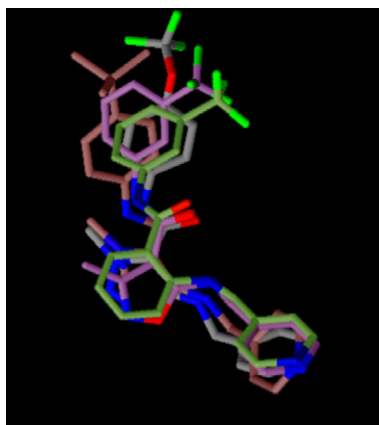


Figure 2. Structural overlap between inhibitor **D** (green) and compounds with the best cellular activities from imidazole (**19**, brown), pyrazole (**43**, gray), and isoxazole (**61**, magenta) series.

compounds. A number of our compounds (**19**, **20**), (**28–30**), and (**33**, **34**) displayed a level of potency that is comparable to that of compounds under clinical development (<100 nM potency in inhibiting cell-based phosphorylation of VEGFR-2). In addition, while some of these compounds displayed mixed VEGFR-1/2 dual activity, others offered VEGFR-2 selectivity. These data suggest that a number of these compounds are good candidates for *in vivo* studies as both VEGFR-2-specific and VEGFR-1/2-dual inhibitors. High permeability of several selected active compounds across Caco-2 cells is predictive of their potential for intestinal absorption upon oral administration (Table 2).

Selected VEGFR-2 inhibitors presented in Table 1 were shown to be ATP-competitive in the radioassay. Competition assays were conducted with varying concentrations (0–100 μM) of ATP. Specifically, five different concentrations of [³²P]ATP were incubated with

Table 2. Passive diffusion potential across Caco-2 cell monolayer for selected compounds

Compound	Intrinsic permeability, P_m value $\times 10^{-5}$ cm/min	Absorption potential
C	38.6 (lit. 45.2) ⁶	High
D	17.3 (lit. 21.7) ⁶	med
5	32.4	High
17	5.7	Low
19	45.3	High
20	37.2	High
27	36.9	High
28	21.6	Med/high
29	42.2	High
30	49.3	High
33	35.6	High
34	42.6	High
43	32.5	Med/high
47	37.5	High
55	40.4	High
60	33.1	Med/high

Table 3. Compounds (**19**), (**34**), and (**43**) are ATP-competitive inhibitors of VEGFR-2

Compound	K_i at IC ₅₀ (μ M)	K_i at IC ₉₀ (μ M)
19	0.20	0.17
34	0.16	0.15
43	0.17	0.18

VEGFR-2 in the absence, IC₅₀ or IC₉₀ concentrations, of the inhibitors for 45 min at RT. A double reciprocal graph of the degree of phosphorylation (1/cpm) against ATP-concentration (1/[ATP]) was plotted. The data were analyzed by a non-linear least-squares program to determine kinetic parameters using *GraphPad* software. Selected K_i values for the three selected compounds are listed in Table 3. Determined K_i values for IC₅₀ or IC₉₀ concentration were compared and found to be identical within experimental error.

In summary, we have developed a series of novel potent *ortho*-substituted azole derivatives active against kinases VEGFR-1 and -2. Both specific and dual ATP-competitive inhibitors of VEGFR-2 were identified. Kinase selectivity could be controlled by varying the arylamido substituent at the azole ring. Compound activities in both enzymatic and cell-based assays (IC₅₀ < 100 nM) were in the range of that for the reported clinical and development candidates, including PTK787 (*Vatalanib*)TM. The analogs presented in this report are potentially useful in the treatment of conditions such as cancer. Further details on their biological properties, such as functional activity, together with murine oral exposure data will be presented in due course.

Acknowledgments

We thank Dr. J. Doody and Dr. Y. Hadari of *ImClone Systems Inc.* for developing enzymatic and cellular assay conditions published in our earlier studies.

References and notes

- (a) Risau, W. *Nature* **1997**, 386, 671; (b) Hanahan, D.; Folkman, J. *Cell* **1996**, 86, 353; (c) Folkman, J.; Klagsburn, M. *Science* **1987**, 235, 442; (d) Folkman, J. *J. Natl. Cancer Inst.* **1991**, 82, 4; (e) Kerbel, E. S. *Carcinogenesis* **2000**, 21, 505.
- (a) Ferrara, N.; Gerber, H.-P.; LeCouter, J. *Nat. Med.* **2003**, 9, 669; (b) Carmeliet, P.; Jain, R. *Nat. Med.* **2003**, 9, 653; (c) Veikkola, T.; Karkkainen, M.; Claesson-Welsh, L.; Alitalo, K. *Cancer Res.* **2000**, 60, 203.
- (a) Klagsbrun, M.; D'Amore, P. *Annual Rev. Physiol.* **1991**, 53, 217; (b) Neufeld, G.; Cohen, T.; Gengrinovitch, S.; Poltorak, Z. *FASEB J.* **1999**, 13, 9; (c) Zachary, I. *Biochem. Soc. Trans.* **2003**, 31, 1171; (d) Klagsbrun, M.; Moses, M. A. *Chem. Biol.* **1999**, 6, R217; The anti-angiogenic antibody *Avastin*TM (Bevacizumab) has recently been approved to treat colorectal cancer, see: (e) Culy, C. *Drugs Today* **2005**, 41, 23; The anti-angiogenic aptamer *Macugen*TM (Pegaptanib sodium) has recently been approved to treat neovascular age-related macular degeneration, see: (f) Fine, S. L.; Martin, D. F.; Kirkpatrick, P. *Nat. Rev. Drug Disc.* **2005**, 4, 187.
- Bold, G.; Altmann, K.-H.; Jorg, F.; Lang, M.; Manley, P. W.; Traxler, P.; Wietfeld, B.; Bruggen, J.; Buchdunger, E.; Cozens, R.; Ferrari, S.; Pascal, F.; Hofmann, F.; Martiny-Baron, G.; Mestan, J.; Rosel, J.; Sills, M.; Stover, D.; Acemoglu, F.; Boss, E.; Emmenegger, R.; Lasser, L.; Masso, E.; Roth, R.; Schlachter, C.; Vetterli, W.; Wyss, D.; Wood, J. M. *J. Med. Chem.* **2000**, 43, 2310.
- (a) Hennequin, L. F.; Stokes, E. S. E.; Thomas, A. P.; Johnstone, C.; Ple, P. A.; Ogilvie, D. J.; Dukes, M.; Wedge, S. R.; Kendrew, J.; Curwen, J. O. *J. Med. Chem.* **2002**, 45, 1300; (b) Wedge, S. R.; Kendrew, J.; Hennequin, L. F.; Valentine, P. J.; Barry, S. T.; Brave, S. R.; Smith, N. R.; James, N. H.; Dukes, M.; Curwen, J. O.; Chester, R.; Jackson, J. A.; Boffey, S. J.; Kilburn, L. L.; Barnett, S.; Richmond, G. H. P.; Wadsworth, P. F.; Walker, M.; Bigley, A. L.; Taylor, S. T.; Cooper, L.; Beck, S.; Juergensmeier, J. M.; Ogilvie, D. J. *Cancer Res.* **2005**, 65, 4389.
- (a) Manley, P. W.; Furet, P.; Bold, G.; Brügggen, J.; Mestan, J.; Meyer, T.; Schnell, C.; Wood, J. *J. Med. Chem.* **2002**, 45, 5697; (b) Manley, P. W.; Bold, G.; Fendrich, G.; Furet, P.; Mestan, J.; Meyer, T.; Meyhack, B.; Strauss, A.; Wood, J. *Cell. Mol. Biol. Lett.* **2003**, 8, 532; (c) Altmann, K.-H.; Bold, G.; Furet, P.; Manley, P. W.; Wood, J. M.; Ferrari, S.; Hofmann, F.; Mestan, J.; Huth, A.; Krüger, M.; Seidelmann, D.; Menrad, A.; Haberey, M.; Thierauch, K.-H., US Patent 6,878,720 B2, **2005**.
- (a) Piatnitski, E. L.; Duncton, M.; Katoch-Rouse, R.; Sherman, D.; Kiselyov, A. S.; Milligan, D.; Balagtas, C.; Wong, W.; Kawakami, J.; Doody, J. *Bioorg. Med. Chem. Lett.* **2005**, 15, 4696; (b) Kiselyov, A. S.; Piatnitski, E. L.; Semenova, M.; Semenov, V. V. *Bioorg. Med. Chem. Lett.* **2006**, 16, 602; (c) Kiselyov, A. S.; Semenova, M.; Semenov, V. V.; Piatnitski, E. L.; Ouyang, S. *Bioorg. Med. Chem. Lett.* **2006**, 16, 2559; (d) Kiselyov, A. S.; Semenova, M.; Semenov, V. V.; Piatnitski, E. L. *Bioorg. Med. Chem. Lett.* **2006**, 16, 1726; (e) Kiselyov, A. S.; Semenova, M.; Semenov, V. V.; Milligan, D. *Bioorg. Med. Chem. Lett.* **2006**, 16, 1913.
- Sobenina, L. N.; Drichkov, V. N.; Mikhaleva, A. I.; Petrova, O. V.; Ushakov, I. A.; Trofimov, B. A. *Tetrahedron* **2005**, 61, 4841.
- Analytical data for selected active compounds: Compound **19**: *N*-(4-*tert*-butylphenyl)-1-methyl-4-(pyridin-4-ylmethylamino)-1*H*-imidazole-5-carboxamide; mp

231–233 °C; ¹H NMR (400 MHz, DMSO-*d*₆) δ, ppm: 1.28 (s, 9H, *t*-Bu), 3.66 (s, 3H, Me), 4.38 (s, 2H, CH₂), 5.28 (br s, exch D₂O, 1H, NH), 7.21 (d, *J* = 7.6 Hz, 2H), 7.48 (d, *J* = 5.6 Hz, 2H), 7.62 (d, *J* = 7.6 Hz, 2H), 8.18 (s, 1H), 8.68 (d, *J* = 5.6 Hz, 2H), 10.25 (br s, exch D₂O, 1H, NH); ¹³C NMR (100 MHz, DMSO-*d*₆) δ, ppm: 29.1, 32.2, 41.2, 46.0, 108.1, 120.9, 123.8, 125.6, 133.0, 138.4, 145.2, 145.8, 147.3, 150.2, 163.4; ESI MS (M+1): 364, (M–1): 362; HRMS, exact mass calcd. for C₂₁H₂₅N₅O: 363.2059; found: 363.2053. Elemental analysis: calcd. for C₂₁H₂₅N₅O: C, 69.40; H, 6.93; N, 19.27; found: C, 69.21; H, 6.76, N, 19.08.

Compound **43**: 1-methyl-4-(pyridin-4-ylmethylamino)-*N*-(4-(trifluoromethoxy)phenyl)-1*H*-pyrazole-5-carboxamide, mp 211–213 °C; ¹H NMR (400 MHz, DMSO-*d*₆) δ, ppm: 3.66 (s, 3H, Me), 4.25 (s, 2H, CH₂), 5.11 (br s, exch. D₂O, 1H, NH), 6.67 (d, *J* = 7.2 Hz, 2H), 7.38 (d, *J* = 5.6 Hz, 2H), 7.60 (d, *J* = 7.2 Hz, 2H), 7.68 (s, 1H), 8.66 (d, *J* = 5.6 Hz, 2H), 10.22 (br s, exch. D₂O, 1H, NH); ¹³C NMR (100 MHz, DMSO-*d*₆) δ, ppm: 34.5, 46.1, 113.9, 121.2, 122.3, 123.6, 127.1, 128.7, 129.4, 133.2, 146.7, 150.2, 157.1, 163.4; ESI MS (M+1): 392, (M–1): 390; HRMS, exact mass calcd. for C₁₈H₁₆F₃N₅O₂: 391.1256; found: 391.1251. Elemental analysis: calcd. for C₁₈H₁₆F₃N₅O₂: C, 55.24; H, 4.12; N, 17.90; found: C, 55.01; H, 4.31; N, 17.76.

Compound **61**: 3-methyl-5-(pyridin-4-ylmethylamino)-*N*-(3-(trifluoromethyl)phenyl)isoxazole-4-carboxamide; mp 196–198 °C; ¹H NMR (400 MHz, DMSO-*d*₆) δ, ppm: 2.29 (s, 3H, Me), 4.35 (s, 2H, CH₂), 5.23 (br s, exch D₂O, 1H, NH), 7.09 (m, 1H), 7.11 (m, 1H), 7.42 (d, *J* = 5.6 Hz, 2H), 7.64 (d, *J* = 7.6 Hz, 1H), 7.75 (d, *J* = 7.6 Hz, 1H), 8.67 (d, *J* = 5.6 Hz, 2H), 10.22 (br s, exch D₂O, 1H, NH); ¹³C NMR (100 MHz, DMSO-*d*₆) δ, ppm: 11.5, 45.3, 99.8, 116.7, 120.5, 123.9, 124.3, 124.8, 125.1, 131.1, 135.7, 147.3, 150.3, 157.6, 158.4, 165.1; ESI MS (M+1): 377, (M–1): 375; HRMS, exact mass calcd. for C₁₈H₁₅F₃N₄O₂: 376.1147; found: 376.1142. Elemental analysis: calcd. for C₁₈H₁₅F₃N₄O₂: C, 57.45; H, 4.02; N, 14.89; found: C, 57.27; H, 3.85; N, 14.76.

- (a) McTigue, M. A.; Wickersham, J. A.; Pinko, C.; Showalter, R. E.; Parast, C. V.; Tempczyk-Russell, A.; Gehring, M. R.; Mroczkowski, B.; Kan, C. C.; Villafranca, J. E.; Appelt, K. *Structure* **1999**, *7*, 319; (b) Berman, H. M.; Westbrook, J.; Feng, Z.; Gilliland, G.; Bhat, T. N.; Weissig, H.; Shindyalov, I. N.; Bourne, P. E. *The Protein Data Bank, Nucleic Acids Res.* **2000**, *28*, 235.
- (a) Hanahan, D.; Folkman, J. *Cell* **1996**, *86*, 353; (b) Folkman, J.; Klagsburn, M. *Science* **1987**, *235*, 442; (c) Zachary, I. *Biochem. Soc. Trans.* **2003**, *31*, 1171; (d) Eskens, F. *Br. J. Cancer* **2004**, *90*, 1.